P-3510

IMAGE FUSION BASED ON WAVELET AND CURVELET TRANSFORM

By

A.KANAGASABAPATHY

Reg. No. 0920107005

of

KUMARAGURU COLLEGE OF TECHNOLOGY

(An Autonomous Institution Affiliated to Anna University of Technology, Coimbatore)

COIMBATORE - 641049

A PROJECT REPORT

Submitted to the

FACULTY OF ELECTRONICS AND COMMUNICATION ENGINEERING

In partial fulfillment of the requirements

for the award of the degree

of

MASTER OF ENGINEERING

IN

COMMUNICATION SYSTEMS

APRIL 2011

BONAFIDE CERTIFICATE

Certified that this project report titled "**IMAGE FUSION BASED ON WAVELET AND CURVELET TRANSFORM**" is the bonafide work of Mr.A.Kanagasabapathy [Reg. No.0920107005] who carried out the research under my supervision. Certified further, that to the best of my knowledge the work reported herein does not form part of any other project or dissertation on the basis of which a degree or award was conferred on an earlier occasion on this or any other candidate.

07.04.2011
Project Guide

Dr.A.Vasuki

Head of the Department

Dr. Rajeswari Mariappan

The candidate with Register No. 0920107005 is examined by us in the project viva-voce examination held on 21/04/2011....

Internal Examiner

21/4/11
External Examiner

ACKNOWLEDGEMENT

First I would like to express my praise and gratitude to the Lord, who has showered his grace and blessing enabling me to complete this project in an excellent manner.

I express my sincere thanks to our beloved Director **Dr.J.Shanmugam**, Kumaraguru College of Technology , for his kind support and for providing necessary facilities to carry out the work.

I express my sincere thanks to our beloved Principal **Dr.S.Ramachandran**, Kumaraguru College of Technology, who encouraged me in each and every steps of the project work.

I would like to express my deep sense of gratitude to our HOD, **Dr.Rajeswari Mariappan**, Department of Electronics and Communication Engineering, for the valuable suggestions and encouragement which paved way for the successful completion of the project work. I also thank her for her kind support and for providing necessary facilities to carry out the work.

In particular, I wish to thank with everlasting gratitude to the project coordinator **D.Mohanageetha(Ph.D).,** Associate Professor, Department of Electronics and Communication Engineering for the expert counseling and guidance to make this project to a great deal of success.

I am greatly privileged to express my heartfelt thanks to my project guide **Dr.A.Vasuki,** Professor, Department of ECE, Kumaraguru College of Technology throughout the course of this project work and I wish to convey my deep sense of gratitude to all the teaching and non-teaching staffs of ECE Department for their help and cooperation.

Finally, I thank my parents and my family members for giving me the moral support and abundant blessings in all of my activities and my dear friends who helped me to endure my difficult times with their unfailing support and warm wishes.

ABSTRACT

Image Fusion is a combination of two or more different images. It extracts the information from multiple source images without any loss in the source images. Wavelet based image fusion is suitable for representing the point singularities in one dimension, but it fails to represent the edges across the curves in two dimensions. This method makes use of curvelet transform based pixel level fusion to detect the discontinuities across the curves. Curvelet transform improves the spatial characteristics and at the same time preserves the frequency characteristics. In curvelet transform operation, the image is decomposed into subbands at various levels using discrete wavelet transform. These sub bands contains both high and low frequencies. A grid of squares is applied on to the subband image to perform smooth partitioning. Then a smooth window function is applied on that square which is followed by renormalizing each square into unit square. Finally inverse transform is applied to get the fused image. The comparison of wavelet and curvelet transform based image fusion is performed. The performance measure like entropy, Root Mean Square and correlation coefficient are evaluated for different fused images.

TABLE OF CONTENTS

CHAPTER NO	TITLE	PAGE NO
	ABSTRACT	iv
	LIST OF TABLES	viii
	LIST OF FIGURES	ix
	LIST OF ABBREVIATIONS	xi
1	INTRODUCTION	1
	1.1 Image Fusion Methods	1
	1.1.1 Linear Superposition	1
	1.1.2 Nonlinear Methods	2
	1.1.3 Optimization Approaches	2
	1.1.4 Image Pyramids	3
	1.1.5 Wavelet Transform	3
	1.1.6 Multiresolution Fusion Scheme	4
	1.2 Project Goal	4
	1.3 Overview	5
	1.4 Organization of the Report	5
2	IMAGE FUSION	6
	2.1 Fusion Approaches	6
	2.2 Image Fusion Levels	6
	2.2.1 Pixel Level Fusion	7
	2.2.2 Feature Level Fusion	7
	2.2.3 Decision Level Fusion	7
	2.3 Types of Image Fusion	8
	2.3.1 Multi-Exposure Image Fusion	8
	2.3.2 Multi-Temporal Image Fusion	8
	2.3.3 Multi-Focus Image Fusion	8

CHAPTER NO	TITLE	PAGE NO
	2.3.4 Multi-Sensor Image Fusion	9
	2.3.5 Medical Image Fusion	9
	2.3.6 Satellite Image Fusion	9
	2.4 Fusion Standards	9
	2.5 Applications of Image Fusion Scheme	10
3	**EXISTING APPROACHES**	**12**
	3.1 Wavelet Transform	12
	3.1.1 Discrete Wavelet Transform	12
	3.1.2 Daubechies Wavelets	12
	3.1.3 Levels of the Transform	14
	3.1.4 Cascading and Filter Banks	15
	3.2 Wavelet Based Image Fusion Schemes	15
	3.2.1 Wavelet Decomposition of Image	18
	3.2.2 Fusion Rule	19
	3.2.3 Wavelet Reconstruction of Image	22
	3.3 Limitations	22
4	**CURVELET TRANSFORM**	**23**
	4.1 Why Curvelet?	23
	4.1.1 Scale Space	24
	4.1.2 Curvelet Transform	25
	4.2 Curvelet Representation	29
	4.3 Continuous Curvelet Transform	30
	4.4 Discrete Curvelet Transform	32
	4.4.1 FDCT-Wrapping	33
	4.4.2 FDCT Architecture	33
	4.4.3 FDCT- Wrapping Algorithm	34
5	**PROPOSED ALGORITHM**	**35**
	5.1 Image Fusion based on DWT and FDCT	35
	5.1.1 Methodology	37

CHAPTER NO	TITLE	PAGE NO
	5.2 Parameters of Evaluation Result	38
	5.3 Experimental Results and Analysis	40
	5.3.1 Multi-focus Image Fusion	40
	5.3.2 Satellite Image Fusion	47
	5.3.3 Complementary Image Fusion	49
6	**CONCLUSION**	**51**
	REFERENCES	**52**

LIST OF TABLES

TABLE NO		PAGE NO
5.1	Evaluation of Multifocus Image Fusion Results	42
5.2	Evaluation of Multifocus Image Fusion Results	44
5.3	Evaluation of Multifocus Image Fusion Results	46
5.4	Evaluation of Satellite Image Fusion Results	48
5.5	Evaluation of Complementary Image Fusion Results	50

CHAPTER 1

INTRODUCTION

With the recent developments in the field of sensing technologies, multisensory systems have become a reality in a growing number of fields such as remote sensing, medical imaging, machine vision and military applications for which they were first developed. The result of these sensing techniques end with an amount of data. Image fusion provides an effective way of reducing this increasing volume of information while at the same time extracting all the useful information from the source images [1].

1.1 IMAGE FUSION METHODS

A generic categorization of image fusion methods is the following:

- Linear Superposition
- Nonlinear Methods
- Optimization Approaches
- Image Pyramids
- Wavelet Transform
- Multiresolution Fusion Scheme

1.1.1 Linear Superposition

The probably most straightforward way to build a fused image of several input frames is performing the fusion as a weighted superposition of all input frames. The optimal weighting coefficients, with respect to information content and redundancy removal, can be determined by a principal component analysis (PCA) of all input intensities. By performing a PCA of the covariance matrix of input intensities, the weightings for each input frame are obtained from the eigenvector corresponding to the largest eigenvalue [2].

A similar procedure is the linear combination of all inputs in a pre-chosen color space leading to a false color representation of the fused image.

1.1.2 Nonlinear Methods

Another simple approach to image fusion is to build the fused image by the application of a simple nonlinear operator such as max or min. If in all input images the bright objects are of interest, a good choice is to compute the fused image by an pixel-by-pixel application of the maximum operator. An extension to this approach follows by the introduction of morphological operators such as opening or closing. One application is the use of conditional morphological operators by the definition of highly reliable 'core' features present in both images and a set of 'potential' features present only in one source, where the actual fusion process is performed by the application of conditional erosion and dilation operators.

A further extension to this approach is image algebra, which is a high-level algebraic extension of image morphology, designed to describe all image processing operations. The basic types defined in image algebra are value sets, coordinate sets which allow the integration of different resolutions and tessellations, images and templates. For each basic type binary and unary operations are defined which reach from the basic set operations to more complex ones for the operations on images and templates. Image algebra has been used in a generic way to combine multisensor images.

1.1.3 Optimization Approaches

In this approach to image fusion, the fusion task is expressed as a bayesian optimization problem. Using the multisensor image data and an a-prior model of the fusion result, the goal is to find the fused image which maximizes the a-posteriori probability. Due to the fact that this problem cannot be solved in general, some simplifications are introduced: All input images are modeled as markov random fields to define an energy function which describes the fusion goal. Due to the equivalence of gibbs random fields and markov random fields, this energy function can be expressed as a sum of so-called clique potentials, where only pixels in a predefined neighborhood affect the actual pixel.

The fusion task then consists of a maximization of the energy function. Since this energy function will be non-convex in general, typically stochastic optimization procedures such as simulated annealing or modifications like iterated conditional modes will be used.

1.1.4 Image Pyramids

Image pyramids have been initially described for multiresolution image analysis and as a model for the binocular fusion in human vision. A generic image pyramid is a sequence of images where each image is constructed by low pass filtering and subsampling from its predecessor. Due to sampling, the image size is halved in both spatial directions at each level of the decomposition process, thus leading to multiresolution signal representation. The difference between the input image and the filtered image is necessary to allow an exact reconstruction from the pyramidal representation. The image pyramid approach thus leads to a signal representation with two pyramids: The smoothing pyramid containing the averaged pixel values, and the difference pyramid containing the pixel differences, i.e. the edges. So the difference pyramid can be viewed as a multiresolution edge representation of the input image. The actual fusion process can be described by a generic multiresolution fusion scheme which is applicable both to image pyramids and the wavelet approach [3].

1.1.5 Wavelet Transform

A signal analysis method similar to image pyramids is the discrete wavelet transform. The main difference is that while image pyramids lead to an over complete set of transform coefficients, the wavelet transform results in a non-redundant image representation. The discrete 2-dim wavelet transform is computed by the recursive application of low pass and high pass filters in each direction of the input image (i.e. rows and columns) followed by subsampling.

One major drawback of the wavelet transform when applied to image fusion is its well-known shift dependency, i.e. a simple shift of the input signal may lead to complete different transform coefficients. This results in inconsistent fused images when invoked in image sequence fusion.

To overcome the shift dependency of the wavelet fusion scheme, the input images must be decomposed into a shift invariant representation. There are several ways to achieve this: The straightforward way is to compute the wavelet transform for all possible circular shifts of the input signal. In this case, not all shifts are necessary and it is possible to develop an efficient computation scheme for the resulting wavelet representation. Another simple approach is to drop

the subsampling in the decomposition process and instead modify the filters at each decomposition level, resulting in a highly redundant signal representation. The actual fusion process can be described by a generic multiresolution fusion scheme which is applicable both to image pyramids and the wavelet approach [4].

1.1.6 Multiresolution Fusion Scheme

The basic idea of the generic multiresolution fusion scheme is motivated by the fact that the human visual system is primary sensitive to local contrast changes, i.e. edges. Motivated from this insight that both image pyramids and the wavelet transform result in multiresolution edge representation, it is straightforward to build the fused image as a fused multiscale edge representation.

The fusion process is summarized in the following: In the first step the input images are decomposed into their multiscale edge representation, using either any image pyramid or any wavelet transform. The actual fusion process takes place in the difference resp. wavelet domain, where the fused multiscale representation is built by a pixel-by-pixel selection of the coefficients with maximum magnitude. Finally the fused image is computed by an application of the appropriate reconstruction scheme [5].

1.2 PROJECT GOAL

The goal of this project is to implement the image fusion scheme based on wavelet and curvelet transform for fusing images like X-ray computed tomography (CT) and magnetic resonance (MRI) images, satellite images and multi focus images. Unlike existing fusion methods, we implement the fusion algorithm based on wavelet and curvelet transform. Curvelet transform represents the images curves, edges and it improves contrast compare to other fusion methods.

1.3 OVERVIEW

The basic steps for image fusion based on wavelet and curvelet transform.

- Reading two sources images and resizes both to same.
- Applying Discrete Wavelet Transform (DWT) to decompose the source images into low pass and high pass sub images and apply curvelet transform on each sub images.
- Applying low pass fusion rules on sub image and finding the low pass fused coefficients.
- Applying high pass fusion rules on sub images and finding the high pass fused coefficients.
- Applying inverse Curvelet Transform and reconstruction algorithm for reconstructing the image from fused high pass and low pass coefficients.
- Performance compare with different parameters.
- The above steps are carried out using MATLAB 7.9.

1.4 ORGANIZATION OF THE REPORT

- **Chapter 2** discusses about the image fusion levels and its operation.
- **Chapter 3** deals about the wavelet transform fundamentals and image fusion based on wavelet transform and its limitations.
- **Chapter 4** deals about the curvelet transform fundamentals and image fusion based on curvelet and wavelet transforms.
- **Chapter 5** gives the implementation steps of the project and discusses the simulation results
- **Chapter 6** shows the Conclusion and Future scope of the project.

CHAPTER 2

IMAGE FUSION

Image fusion is the process by which two or more images are combined into a single image, retaining the important features from each of the original images. The goal of Image Fusion is to integrate complementary multi-sensor, multitemporal and/or multi-view information into one new image, the quality of which cannot be achieved otherwise. The term "quality", its meaning and measurement depend on the particular application. An image contains different types of information. The objective in image fusion is to increase information that is relevant to a particular application.

2.1 FUSION APPROACHES

Any image fusion methodology consists of two basic stages: image registration, which brings the input images to spatial alignment, and fusion itself, i.e., combining image functions (intensities, colors, etc.) in the area of frame overlap. Several approaches to image fusion can be distinguished, depending on whether the images are fused in the spatial domain or they are transformed into another domain, and their transforms fused.

Image fusion has been used in many application areas. In remote sensing and in astronomy, multisensor fusion is used to achieve high spatial and spectral resolutions by combining images from two sensors, one of which has high spatial resolution and the other one high spectral resolution. Numerous fusion applications have appeared in medical imaging like simultaneous evaluation of CT, MRI, and/or Positron Emission Tomography (PET) images [6].

2.2 IMAGE FUSION LEVELS

Image fusion algorithms can be categorized into low, mid, and high levels. In some literature, this is referred to as

- Pixel Level or Signal level image Fusion
- Feature level Image Fusion
- Symbol or Decision Level Image Fusion.

2.2.1 Pixel Level Fusion

It is a low level fusion scheme and also a nonlinear method. In this fusion scheme intensity value of pixel of the source Images are used for merging the images.

Most of the fusion techniques are used pixel level fusion scheme. Because, in this scheme provided output image closer to original image. It provides stereo viewing capability for stereo photogram try. It substitutes missing data. This fusion scheme dose not introduces any inconsistencies. A typical pixel-level image fusion system can be divided into six subsystems: imaging, registration, pre- processing, fusion, post-processing and displaying [7].

2.2.2 Feature Level Fusion

It is a mid-level fusion technique. This scheme operates on characteristics of source images such as size, shape, edge and mutual information. Feature-level fusion is performed via the detection or extraction of the useful features with a certain level of confidence. It is suitable when different type of sensors measure different phenomena or features. The features in one modality are matched into the corresponding features of another modality. Generally, feature-level fusion does not require as much strict registration as the pixel-level fusion. Gauss-Markov random fields are a commonly used method to minimize total energy consumption during the feature-level data fusion [8].

2.2.3 Decision Level Fusion

It is a high level fusion technique. It deals with symbolic representation of image. Decision-level fusion is a way allowing the information from multiple sensors to be effectively used at the higher level of abstraction. It is often employed in the applications where sensors are deployed at different regions of environments. Simultaneous detection of lane and pavement boundaries is the widely used application of symbol-level fusion. It captures and passes a binary "match/no-match" vector decision model. Fusion is based on majority scheme. In this fusion scheme there is a chance to loss the data. So this scheme is not use popularly.

2.3 TYPES OF IMAGES FUSION

2.3.1 Multi Exposure Image Fusion

The real world scenes exhibit very high dynamic ranges in luminosity, color and focus. Fortunately the HVS is capable of efficiently capturing and presenting these images to the human brain which is able to efficiently fuse these images, creating a very high degree of realism. Unfortunately traditional digital cameras are limited in their capability as they cannot capture the whole dynamic range of luminosity, color and focus of the real world scenes in a single shot. Each image of the multiple set of images consists of a certain area that is better exposed or focused as compared to the same area in all other images. By separating and combining these areas, a visually optimized representation of the complete image can be obtained [9].

2.3.2 Multi Temporal Image Fusion

Temporal Image fusion integrates simultaneously spatial and temporal evolution of the tracer revealing information that cannot be perceived in an image of one time sequence. Usually dynamic studies are performed by drawing manually regions of interest (ROI) on an image. This image is chosen from different time acquisitions for showing the optimal contrast for the given ROI. Then the average value of the pixels belonging to this ROI is collected for each sequence time and the kinetic parameters are injected in a bio-mathematical mode relevant data from the measurement [10].

2.3.3 Multi Focus Image Fusion

Due to the limited focus depth of the optical lens, it is often not possible to get an image that contains all relevant objects in focus. In an image captured by those devices, only those objects within the depth of field are focused, while other objects are blurred. To obtain an image with every object in focus, a multi-focus image fusion process is required to fuse the images taken from the same view point under different focal settings. The fused image gives a better view for human or machine perception

2.3.4 Multi Sensor Image Fusion

The information science research associated with the development of sensory systems focuses mainly on how information about the world can be extracted from sensory data. The sensing process can be interpreted as a mapping of the state of the world into a set of much lower dimensionality. The mapping is many to one which means that there are typically many possible configurations of the world that may give rise to the measured sensory data. Thus, in many cases, a single sensor is not enough to provide an accurate perception of the real world.

2.3.5 Medical Image Fusion

In medical, CT and MRI image both are topographic scanning images and have different features. In CT image brightness is related to tissue density. So the brightness of bone is higher and some of soft tissue can't be seen in CT images. In MRI image brightness is related to amount of hydrogen atom in tissues, thus brightness of soft tissue is higher, and bones can't be seen. By using fusion technique, it can be possible to get both information in the single output image.

2.3.6 Satellite Image Fusion

Large number of images is provided by satellite with different spatial resolution and spectral resolution. In the color image fusion two different characteristics of images are fused. High spatial resolution panchromatic image (poor spectral resolution) and lower spatial resolution multispectral image (high spectral resolution) are fused. In this type of image fusion improve and have high quality color components than original image .This type of fusion is used in remote sensing field to obtain high spatial resolution with high spectral resolution image.

2.4 FUSION STANDARDS

- **Simple Average**: It is a well-documented fact that regions of images that are in focus tend to be of higher pixel intensity. Thus this algorithm is a simple way of obtaining an output image with all regions in focus. The value of the pixel P (i, j) of each image is taken and added. This sum is then divided by N to obtain the average. The average value

is assigned to the corresponding pixel of the output image. This is repeated for all pixel values.

- **Simple Greatest Pixel:** The greater the pixel values the more in focus the image. Thus this algorithm chooses the in-focus regions from each input image by choosing the greatest value for each pixel, resulting in highly focused output. The value of the pixel P (i, j) of each image is taken and compared to each other. The greatest pixel value is assigned to the corresponding pixel of the output image. This is repeated for all pixel values.
- **Simple Block Replace:** Unlike the two previous algorithms, this algorithm takes into consideration the neighboring pixels for each pixel. For each pixel P (i, j) of each image its neighboring pixels are added and a block average is calculated. After comparison, the pixel from the input image with the maximum block average is copied to the output image. This is repeated for all pixel values.
- **Wavelet Decomposition and Reconstruction:** Two-dimensional Discrete Wavelet Transform (DWT) leads to a decomposition of approximation coefficients at level j in four components: the approximation at level j + 1, and the details in three orientations (horizontal, vertical, and diagonal). This gives a level 1 decomposed image.

2.5 APPLICATIONS OF IMAGE FUSION SCHEME

Image fusion is widely recognized tool for improving overall system performance in image based applications areas such as defense surveillance, remote sensing, medical imaging and computer vision.

Intelligent robots

- Require motion control, based on feedback from the environment from visual, tactile, force/torque, and other type of sensors.
- Stereo camera fusion.
- Intelligent viewing protocol.
- Automatic target recognition and tracking.

Medical Image

- Fusing X-ray Computed Tomography (CT) and Magnetic Resonance Images (MRI)
- Computer assisted surgery
- Spatial registration of 3-D surface

Manufacturing

- Electronic circuit and component inspection
- Product surface measurement and inspection
- Non-destructive material inspection
- Complex machine/device diagnostics
- Intelligent robots on assembly lines

Military and law enforcement

- Detection, tracking, identification of ocean (air, ground) target/event
- Concealed weapon detection
- Battle-field monitoring
- Night pilot guidance

Remote sensing

- Using various parts of the electro-magnetic spectrum
- Sensors: from black-and-white aerial photography to multi-spectral active microwave space-borne imaging radar

This chapter describes clearly the methods and level of image fusion. Also, the application of image fusion in various fields is presented in this chapter. The existing approaches in the image fusion are given in the following chapter.

CHAPTER 3

EXISTING APPROACHES

3.1 WAVELET TRASFORM

In mathematics, a wavelet series is a representation of a square-integral (real- or complex-valued) function by a certain orthonormal series generated by a wavelet. This article provides a formal, mathematical definition of an orthonormal wavelet and of the integral wavelet transform. There are two types of wavelet transform DWT and CWT.

3.1.1 Discrete Wavelet Transform

Discrete wavelet transform (DWT) is any wavelet transform for which the wavelets are discretely sampled. As with other wavelet transforms, a key advantage it has over Fourier transforms is temporal resolution: it captures both frequency and location information.

The first DWT was invented by the Hungarian mathematician Alfred Haar. For an input represented by a list of 2^n numbers, the Haar wavelet transform may be considered to simply pair up input values, storing the difference and passing the sum. This process is repeated recursively, pairing up the sums to provide the next scale: finally resulting in $2^n - 1$ differences and one final sum.

3.1.2 Daubechies Wavelets

The most commonly used set of discrete wavelet transforms was formulated by the Belgian mathematician Ingrid Daubechies in 1988. This formulation is based on the use of recurrence relations to generate progressively finer discrete samplings of an implicit mother wavelet function; each resolution is twice that of the previous scale. In her seminal paper, Daubechies derives a family of wavelets, the first of which is the Haar wavelet. Interest in this field has exploded since then, and many variation ns of Daubechies' original wavelets were developed.

The Daubechies wavelets are a family of orthogonal wavelets defining a discrete wavelet transform and characterized by a maximal number of vanishing moments for some given support. With each wavelet type of this class, there is a scaling function (also called father wavelet) which generates an orthogonal multiresolution analysis.

In general, the Daubechies wavelets are chosen to have the highest number A of vanishing moments, for given support width N=2A, and among the 2^{A-1} possible solutions .The one is chosen whose scaling filter has extremely phase. The wavelet transform is also easy to put into practice using the fast wavelet transform. Daubechies wavelets are widely used in solving a broad range of problems, e.g. self-similarity properties of a signal or fractal problems, signal discontinuities, etc.

Daubechies orthogonal wavelets D2-D20 (even index number only) are commonly used. The index number refers to the number N of coefficients. Each wavelet has a number of zero moments or vanishing moments equal to half the number of coefficients. For example, D2 has one vanishing moment, D4 has two, etc. A vanishing moment limits the wavelet's ability to represent polynomial behavior or information in signal.

For example, D2, with one moment, easily encodes polynomials of one coefficient, or constant signal components. D4 encodes polynomials with two coefficients, i.e. constant and linear signal components; D6 encodes 3-polynomials, i.e. constant, linear and quadratic signal components. This ability to encode signals is nonetheless subject to the phenomenon of scale leakage, and the lack of shift-invariance, which arise from the discrete shifting operation during application of the transform.

Sub-Sequence which represent linear, quadratic signal components are treated differently by the transform depending on whether the points align with even-or-odd- numbered locations in the sequence. The lack of the important property of shift-invariance, has led to the development of several different versions of a shift-invariant wavelet transform.

3.1.3 Levels Of The Transform

- **One level of the transform:** The samples are passed through a low pass filter with impulse response g resulting in a convolution of the two

$$y[n] = (x * g)[n] = \sum_{k=-\infty}^{\infty} x[k]g[n-k] \qquad \text{--------} (3.1)$$

The signal is also decomposed simultaneously using a high-pass filter h. The outputs giving the detail coefficients (from the high-pass filter) and approximation coefficients (from the low-pass). It is important the two filters are related to each other and they are known as a quadrature mirror filter. However, since half the frequencies of the signal have now been removed, half the samples can be discarded according to Nyquist's rule. The filter outputs are then sub sampled by 2 (Mallat's and the common notation is the opposite, g- high pass and h- low pass)

$$y_{low}[n] = \sum_{k=-\infty}^{\infty} x[k]g[2n-1] \qquad \text{--------} (3.2)$$

$$y_{high}[n] = \sum_{k=-\infty}^{\infty} x[k]h[2n+1-k] \qquad \text{--------} (3.3)$$

This decomposition has halved the time resolution since only half of each filter output characterizes the signal. However, each output has half the frequency band of the input so the frequency resolution has been doubled.

3.1.4 Cascading And Filter Banks

This decomposition is repeated to further increase the frequency resolution and the approximation coefficients decomposed with high and low pass filters and then down-sampled. This is represented as a binary tree with nodes representing a sub-space with different time-frequency localization. The tree is known as a filter bank.

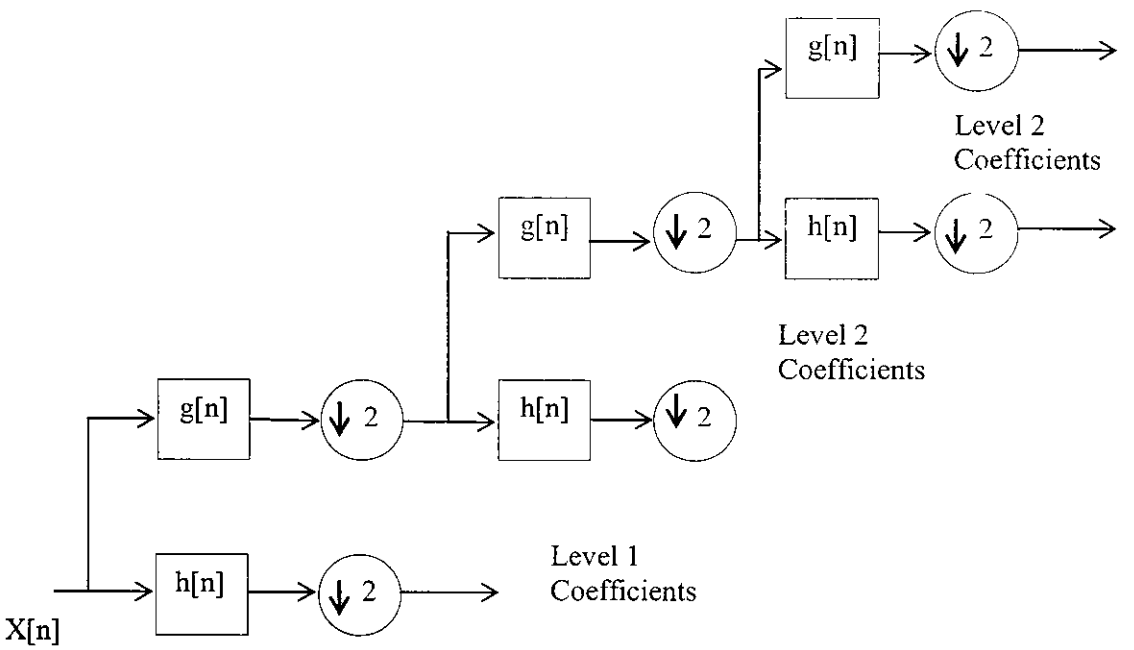

Fig 3.1 Cascading and Filter Banks

3.2 WAVELET BASED IMAGE FUSION SCHEMES

The general procedure of wavelet-based image fusion algorithm is shown in Fig. 3.1. Where I_1 and I_2 denote the source images to be fused, and are assumed to be well registered. L denotes the wavelet decomposition level. F is the final fused image. I_1, and I_2 are first decomposed by the Lth level wavelet transform into 3L horizontal, vertical and diagonal detail sub-images at each of the L resolution levels and a gross approximation of the image at the coarsest resolution level. Haar wavelet transformation is used. Couple sub images of I_1, and I_2

are then combined, respectively. The final fused image is reconstructed by inverse wavelet transform from the modified coefficients. The algorithms will be discusses as follows in detail

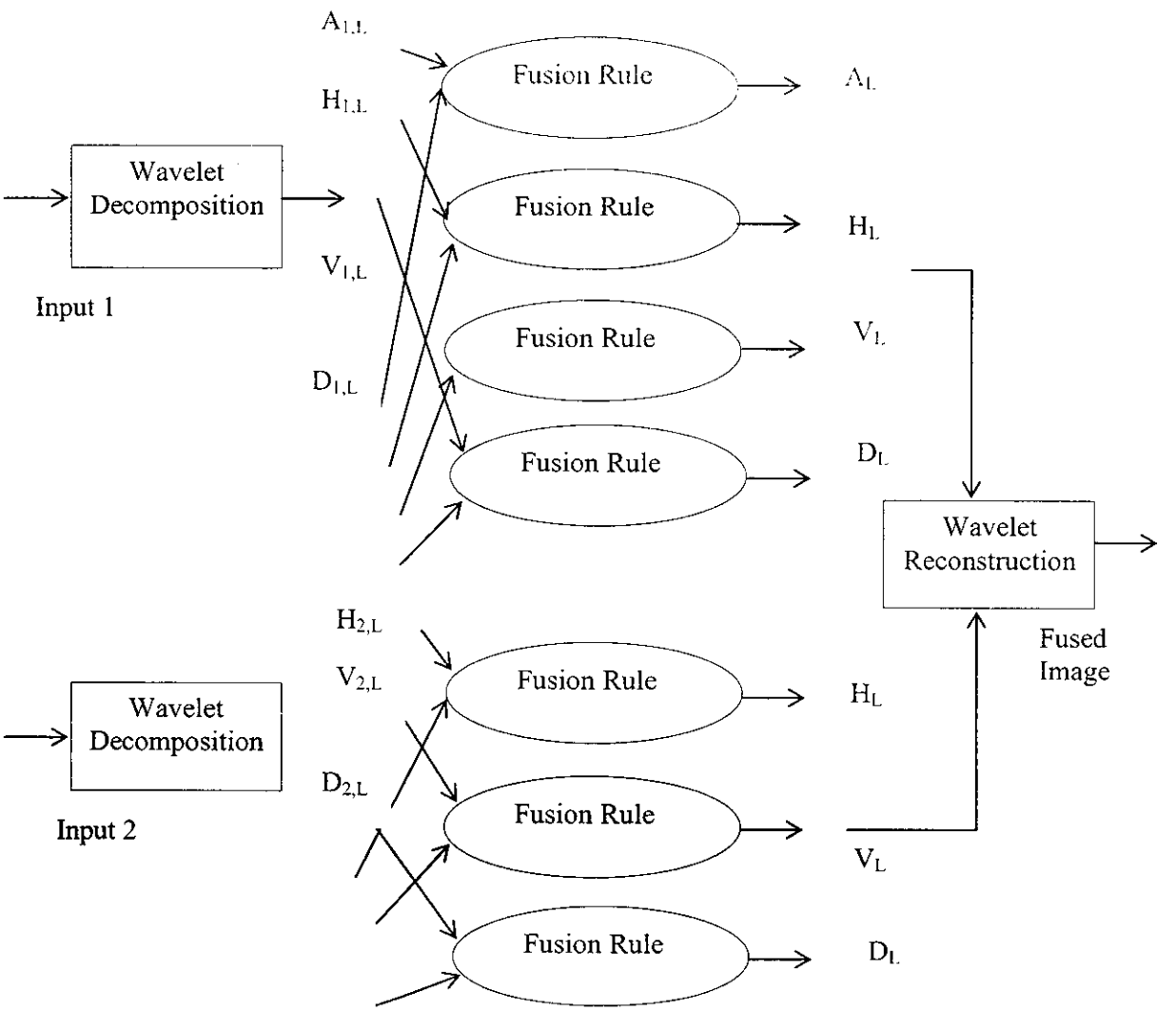

Fig.3.2 General Wavelet based Image Fusion Procedure

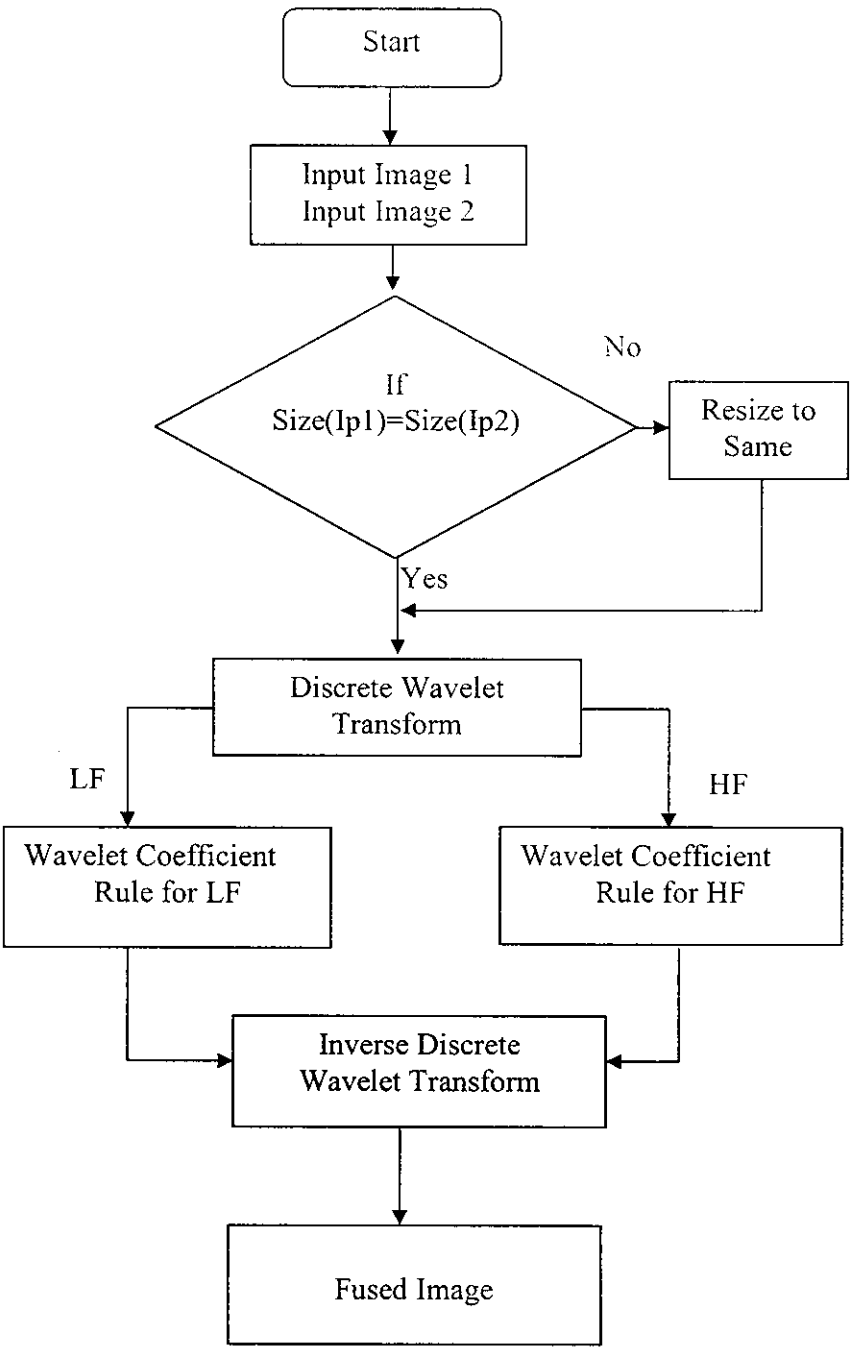

Fig.3.3 Wavelet Based Image Fusion

3.2.1 Wavelet Decomposition of Image

Wavelet decomposition of image is two directional filtering operations and subsampling by a factor of two. Since the scaling and wavelet function are separable, image decomposition can be computed with a separable extension of the one-dimensional decomposition on the rows and columns. At each stage of transform, the image is decomposed into four images. Taking image as an example, at the stage of wavelet transform, it is decomposed into four sub images and as shown in Figure 3.2. The first component, which is gotten by twice low-passed filtering is named low frequency component (also called a gross approximation) and it will be the original image of next transform. It contains the horizontal, vertical, and diagonal high frequency information respectively. In Figure 3.2, H is a low-passed filter; G is a high-passed filter [12].

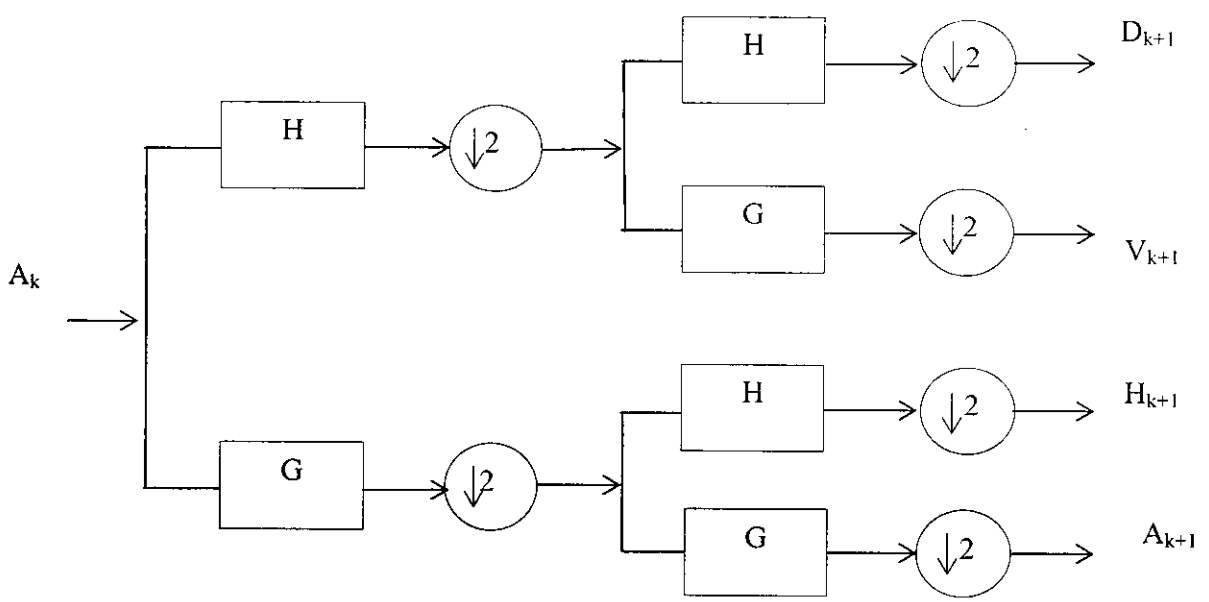

Fig. 3.4 Wavelet Decomposition of an Image

All of the source images are transformed into the Lth level wavelet domain to produce a sequence of 3L detail images corresponding to the horizontal, vertical and diagonal details at each of the L resolution levels, and a gross approximation of the image at the coarsest resolution level.

3.2.2 Fusion Rule

The fusion algorithm is decided according to the goal of fusion. When the details of the image are to be retained, pick up these corresponding coefficients to reconstruct the result image. When the goal is to restrain the noise, set the corresponding coefficients to zero, then reconstruct the image. In this paper, the impact factors of clouds and its shadows on the ground are the primary to be eliminated; meanwhile the details should be retained [11].

For the horizontal, vertical and diagonal detail images, the fusion algorithm uses two distinct methods of merging, i.e. selection and averaging. In this algorithm, salient features in each source image are identified, and have an effect on the composite image. The salience feature is defined as a local energy in the neighborhood of a coefficient.

$$S(x,y,k) = \sum_{m} \sum_{n} C(x + m, y + n, k)^2 \qquad \text{-------- (3.4)}$$

where (x,y) is the location of the current wavelet coefficient, k is the decomposition level, c(x,y,k) is the current wavelet coefficient at location (x,y) ($cH_{j,k}$, $cV_{j,k}$ or $cD_{j,k}$), and (m,n) defines a window of coefficients around the current coefficient. The size of the window is typically small, e.g. 3 by 3.

At a given resolution level (Hj,k, $V_{j,k}$ and $D_{j,k}$, j =1,2, k=1, ...L), the image fusion algorithm uses a matching measure that determines the methods of merging. The matching measure at position (x, y) and decomposition level k is defined as

$$M(x,y,k) = \frac{2\sum_{m}\sum_{n} C_1(x+m, y+n, k) C_2(x+m, y+n, k)}{S_1(x,y,k) + S_2(x,y,k)} \qquad \text{-------- (3.5)}$$

Where subscripts 1 and 2 refer to the source images I_1 and I_2 respectively. M is used to compare with a threshold T_1 (e.g. 0.5) to determine whether selection or averaging will be used.

If M is less than or equal to T_1, the coefficient with the largest salience is substituted for the composite transform while the less salient coefficient is discarded. The selection mode is implemented as

$$C(x,y,k) = \begin{Bmatrix} C_1(x,y,k).if S_1(x,y,k) \geq S_2(x,y,k) \\ C_2(x,y,k).if S_1(x,y,k) \leq S_2(x,y,k) \end{Bmatrix}$$

-------- (3.6)

where c(x, y,k) are the final fused coefficients in the composite wavelet transform (cH_k, cV_k, cD_k, k=1, ...L)

If M is greater than T_1, the source images are more similar and the weighted average is calculated from the coefficients of both source transforms. The weights used for averaging are defined as

$$\omega_{\min} = \frac{M - \alpha}{2(1-\alpha)}$$
$$\omega_{\max} = 1 - \omega_{\min}$$

-------- (3.7)

where ω_{min} is applied to coefficient with lower salience while ω_{max} is applied to the coefficient with higher one. In the averaging mode, the composite transform coefficient is the weighted average of the source coefficients and is implemented as

$$C(x,y,k) = \begin{Bmatrix} \omega_{\max}(x,y,k).C_1(x,y,k) + \omega_{\min}(x,y,k).C_2(x,y,k) if S_1(x,y,k) \geq S_2(x,y,k) \\ \omega_{\min}(x,y,k).C_1(x,y,k) + \omega_{\max}(x,y,k).C_2(x,y,k) if S_1(x,y,k) \leq S_2(x,y,k) \end{Bmatrix}$$

-------- (3.8)

At the coarsest resolution level, the matching measure is also identified and used to determine the method of combination of coefficients, i.e. selection or averaging. The matching

measure is calculated according to (1) and (2), but the selection and averaging algorithms of the coefficients are different to that of the high frequency detail images. M is used to compare with a threshold T_1 (e.g. 0.7) to determine whether selection or averaging will be used.

If M is greater than T_2, the source images are more similar and the average is calculated from coefficients of both source transforms. The composite transform coefficient are given by

$$cA_L(x,y) = \frac{1}{2}(cA_{1,L}(x,y) + C_{2,L}(x,y))$$

-------- (3.9)

If M is less than or equal to T_2, the coefficient with high energy is substituted for the composite transform while the coefficient with low energy is discarded. The high details of A are given by

$$A_j(x,y) = A_{j,L}(x,y) - A_{j,L+1}(x,y), j = 1,2..$$

-------- (3.10)

The local energy of the coefficient in location (x,y) defined as

$$E_j(x,y) = \sum_m \sum_n p(m,n) A_j(x+m, y+n)$$

-------- (3.11)

where operator p(m,n) is given by {{0,1,0},{1,2,1}, {0,1,0}. The coefficient with higher energy is substituted for the composite transform while the lower energy coefficient is discarded. The selection mode is implemented as

$$c(x,y) = \begin{Bmatrix} cA_{1,L}(x,y), if E_1(x,y) \geq E_2(x,y) \\ cA_{2,L}(x,y), if E_1(x,y) \leq E_2(x,y) \end{Bmatrix}$$

-------- (3.12)

After all of the coefficients in the composite wavelet representation are obtained, the inverse wavelet transform is performance to get the final fused image [13].

3.2.3 Wavelet Reconstruction of an Image

The final fused image is reconstructed by performing the inverse wavelet transform from the fused wavelet coefficients. On the contrary to wavelet decomposition, the inverse wavelet transform, or wavelet reconstruction, is a up-sampling and restoration operation. This process is diagrammed in Figure 3.3. in which H and G are reversed filter of H and G, respectively.

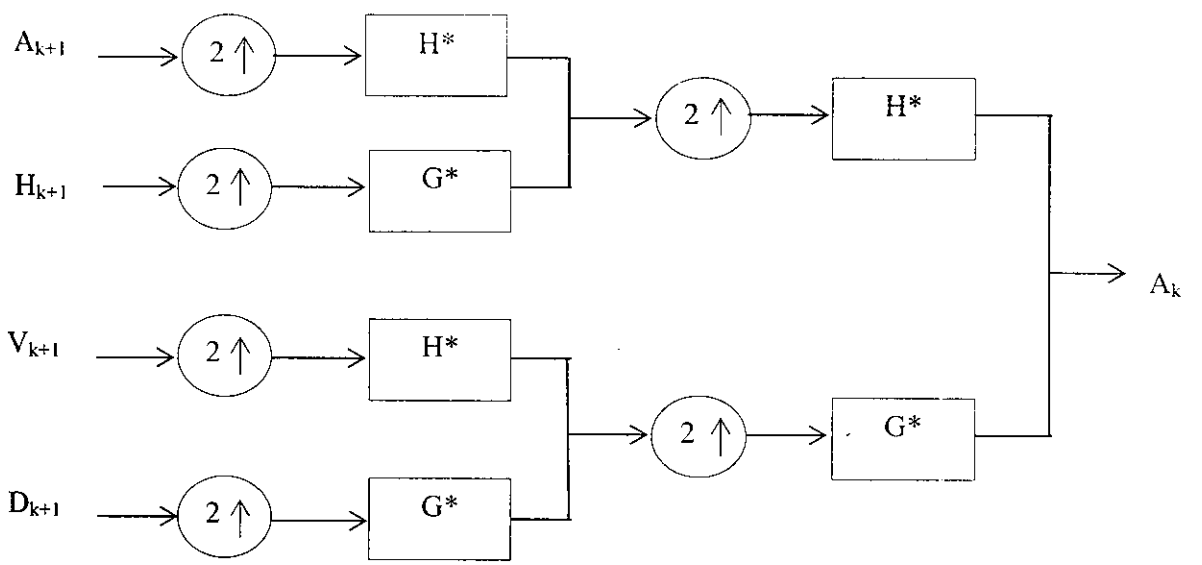

Fig.3.5 Wavelet Reconstruction of an Image

3.3 LIMITATIONS

- The edges and singularities are not well represented
- Suffers from limited directionality
- The point singularity is better suited for wavelets in 1D signals ,but 2D signals like images have curve or line singularities where wavelets fails to approximate.
- DWT is not a suitable transform for edge information.

The discrete wavelet transforms and its based image fusion scheme is discussed in this chapter. The curvelet transform and its applications are given in the following chapter.

CHAPTER 4

CURVELET TRANSFORM

Efficient representation of images can be achieved by transforms. However, conventional transforms such as Fourier transform and wavelet transform suffer from discontinuities such as edges in images. To address this problem, a new transform called curvelet transform. Curvelet Transform was proposed by Candes and Donoho in 2000, it derived from Ridgelet Transform The curvelet transform is a higher dimensional generalization of the ridgelet transform, designed to represent images or two-dimensional signals at different scales and different directions [14].

4.1 WHY CURVELET?

Efficient representation of images or signals is critical for image processing, computer vision, and pattern recognition and image compression. Harmonic analysis provides a methodology to represent signals efficiently. Specifically, harmonic analysis is intended to efficiently represent a signal by a weighted sum of basic functions; here the weights are called coefficients and the mapping from the input signal to the coefficients is called transform. In image processing, Fourier transform is usually used. However, Fourier transform can only provide an efficient representation for smooth images but not for images that contain edges. Edges or boundaries of objects cause discontinuities or singularities in image intensity.

How to efficiently represent singularities in images poses a great challenge to harmonic analysis. It is well known that one-dimensional (1D) singularities in a function (which has finite duration or is periodic) destroy the sparsity of Fourier series representation of the function, which is known as Gibbs phenomenon [15]. In contrast, wavelet transform is able to efficiently represent a function with 1D singularity. However, typical wavelet transform is unable to resolve two-dimensional (2D) singularities along arbitrarily shaped curves since typical 2D wavelet transform is just a tensor product of two 1D wavelet transforms, which resolve 1D horizontal and vertical singularity, respectively.

To overcome the limitation of wavelet, ridgelet transform was introduced. Ridgelet transform can resolve 1D singularity along an arbitrary direction (including horizontal and

vertical direction). Ridgelet transform provides information about orientation of linear edges in images since it is based on Radon transform, which is capable of extracting lines of arbitrary orientation. Since ridgelet transform, is not able to resolve 2D singularities, Candes and Donoho proposed the first generation curvelet transform based on multi-scale ridgelet. Later, they proposed the second generation curvelet transform. Curvelet transform can resolve 2D singularities along smooth curves. Curvelet transform uses a parabolic scaling law to achieve anisotropic directionality [16]. From the perspective of micro local analysis, the anisotropic properties of curvelet transform guarantees resolving 2D singularities along C2 curves. Ridgelet transform Type I generalizes curvelet transform by adding two parameters, i.e., support c and degree d; hence, curvelet transform is just a special case of ridgelet transform Type I with c = 1 and d = 2. The new parameters, i.e., support c and degree d, provide ridgelet transform with anisotropy capability of representing singularities along arbitrarily shaped curves.

4.1.1 Scale Space

A thing about mathematical transforms is that they may be applied to a wide variety of problems as long as they have a useful architecture. The Fourier transform, for example, is much more than a convenient tool for studying the heat equation (which motivated its development) and, by extension, constant-coefficient partial differential equations. The Fourier transform indeed suggests a fundamentally new way of organizing information as a superposition of frequency contributions, a concept which is now part of our standard repertoire. In a different direction, we mentioned before that wavelets have flourished because of their ability to describe transient features more accurately than classical expansions. Underlying this phenomenon is a significant mathematical architecture that proposes to decompose an object into a sum of contributions at different scales and locations. This organization principle, sometimes referred to as scale-space, has proved to be very fruitful - at least as measured by the profound influence it bears on contemporary science.

Curvelet also exhibit an interesting architecture that sets them apart from classical multiscale representations. Curvelet partitions the frequency plane into dyadic coronae and (unlike wavelets) sub partition those into angular wedges which again display the parabolic aspect ratio. Hence, the curvelet transform refines the scale-space viewpoint by adding an extra element, orientation, and operates by measuring information about an object at specified scales

and locations but only along specified orientations. The specialist will recognize the connection with ideas from micro local analysis. The joint localization in both space and frequency allows us to think about curvelet as living inside "Heisenberg boxes" in phase-space, while the scale/location/orientation discretization suggests an associated tiling (or sampling) of phase-space with those boxes. Because of this organization, curvelet can do things that other systems cannot do.

For example, they accurately model the geometry of wave propagation and, more generally, the action of large classes of differential equations: on the one hand they have enough frequency localization so that they approximately behave like waves, but on the other hand they have enough spatial localization so that the flow will essentially preserve their shape [17].

4.1.2 Curvelet Transform

A brief overview of the mathematical framework from is now presented to give the reader a formal representation of curvelets. Each curvelet is defined by three parameters (j,k,l).

Where,

j = scale

l = orientation

k = location

- Parabolic Scaling Matrix:

$$D_j = \begin{pmatrix} 2^{2j} & 0 \\ 0 & 2^j \end{pmatrix}$$

-------- (4.1)

- Rotation Angle:

$$\theta_J = 2\pi * 2^{-J} * l$$

-------- (4.2)

➢ Translation Parameter:

$$k_{\delta} = (k_1 * \delta_1, k_2 * \delta_2)$$
$$\delta_1, \delta_2 = \text{normalizng constants} \qquad \text{-------- (4.3)}$$

➢ Curvelet Basis Function:

$$\gamma(x_1, x_2) = \psi(x_1) * \phi(x_2)$$
$$\psi(x_1) = Gabor\,(x_1) \qquad \text{-------- (4.4)}$$
$$\phi(x_2) = Gaussian\,(x_2)$$

Finally, the curvelet parameterized by (j,k,l) can be defined as

$$\gamma_{(j,l,k)}(x_1, x_2) = 2^{\frac{3j}{2}} * \gamma(D_J * R_{\theta_J} * (x_1, x_2) - k_{\delta})$$

-------- (4.5)

➢ Curvelet Properties:

- **Anisotropy Scaling Law**: The general scaling and support result in anisotropy of curvelet functions, which guarantees to capture singularities along various curves.
  - Width ~ length^2

- **Directional Sensitivity**: curvelet functions orient at various directions. With the increasing of resolution, curvelet functions can obtain more directions.
  - Orientations = 1/j

- **Spatial Localization:** Curvelet coefficients form a Cartesian coordinate grid with spacing proportional to the length in θ_j direction and the width of the curvelet in the normal (respective to θ_j) direction

- **Oscillatory Nature**: Across a ridge, a curve displays an oscillatory nature. Curvelet functions have compact support in frequency domain and decay very fast in spatial domain. So curvelet functions are well localized in both spatial and frequency domains.

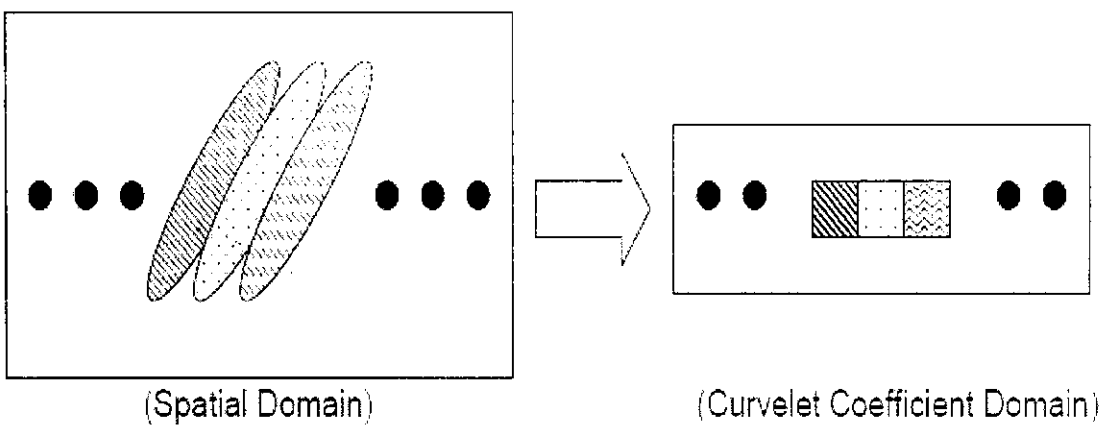

Fig. 4.1 A Group of Curvelets at a Fixed Orientation and Scale and its Relationship to the Curvelet Transform.

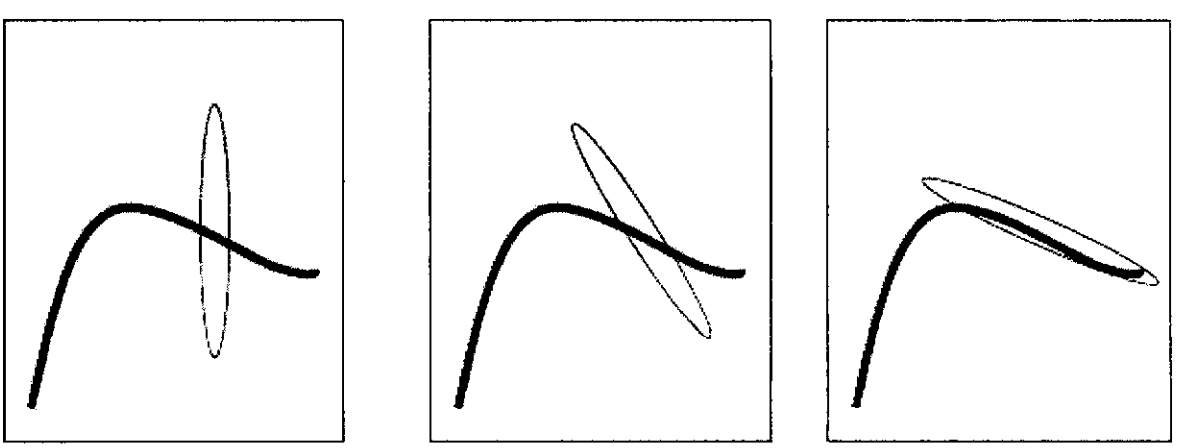

Fig. 4.2 Example of Curvelets with Fixed Scale and Location, Varying along Orientation

Using curvelets of varying orientation (Figure above) the resulting coefficients would be very close to zero for Fig.4.2(a) due to only a small amount of edge energy included in the curvelet area. Fig.4.2(b) would have a slightly larger coefficient but still relatively small in comparison to the coefficient related to figure Fig.4.2(c) which would be quite large due to the tight frame of the curvelet being tangential to the edge.

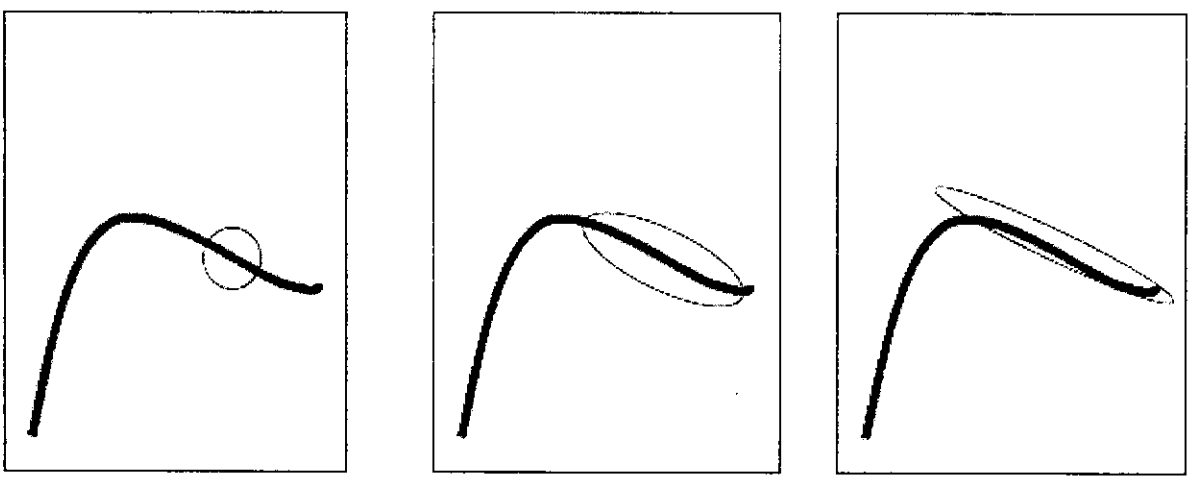

(a) (b) (c)

Fig. 4.3 Example of Curvelets with Fixed Orientation and Location, Varying across Scale

Using curvelet of varying scale aligned with an edge (Figure), one can see how the changes in scale will affect the resulting coefficient. For a coarse scale decomposition Fig.4.3 (a), the curvelet coefficient resulting will be of moderate size due to the frame being tangential to the edge, but would contain a large amount of area without any edge energy. The medium scale decomposition Fig 4.3(b) will be larger due to the length of the curvelet having increased therefore containing more of the edge. The fine scale representation Fig.4.3(c) will result in the largest coefficient due to almost the entire curvelet frame being filled with the edge energy.

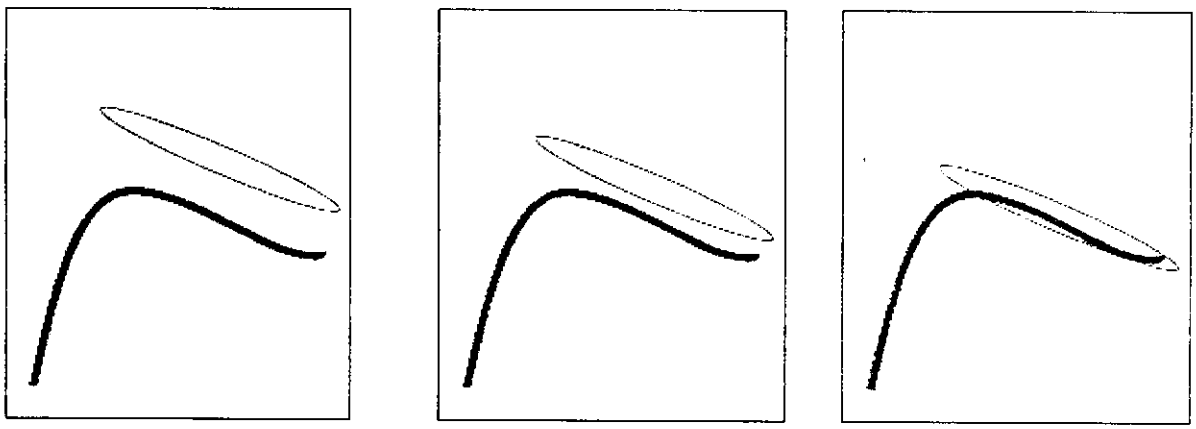

(a) (b) (c)

Fig. 4.4 Example of Curvelets with Fixed Orientation and Scale, Varying across Location

Using curvelets of varying location the strength of the algorithm becomes obvious as Figures (a) and (b) would result in a coefficient very close to zero (curvelets are not compactly supported), while the coefficient related to Fig (c) would be very large due to the edge being contained in the curvelet frame.

4.2 CURVELET REPRESENTATION

When performing the curvelet transform on a C^2 curve, very few curvelet coefficients will be above negligible magnitude values. In, it is declared that curvelets offer optimal sparseness for "curve-punctuated smooth" images, where the image is smooth with the exception of discontinuities along C^2 curves. Sparseness is measured by the rate of decay of the m-term approximation (reconstruction of the image using m number of coefficients) of the algorithm. Having a sparse representation, along with offering improved compression possibilities, also allows for improving denoising performance as additional sparseness increases the amount of smooth areas in the image.

The orthogonal systems have optimal m-term approximations that decay in L^2 with rate O (m^{-2}) (as a lower bound). Currently, there does not exist a single computationally feasible transform that will obtain this lower bound.

On images with C^2 boundaries, non-optimal systems have the rates:

- **Fourier Approximation:**

$$\left\| f - f_m^F \right\|_{L_2}^2 \approx O(m^{-1/2}) \qquad \text{------ (4.6)}$$

- **Wavelet Approximation:**

$$\left\| f - f_m^F \right\|_{L_2}^2 \approx O(m^{-1}) \qquad \text{------ (4.7)}$$

- **Curvelet Approximation:**

$$\left\| f - f_m^F \right\|_{L_2}^2 \approx O((\log\ m)^3\, m^{-1}) \qquad \text{------ (4.8)}$$

As seen from the m-term approximations, the Curvelet Transform offers the closest m-term approximation to the lower bound. Therefore, in images with a large number of C^2 curves (i.e. an image with a great number of long edges), it would be advantageous to use the Curvelet Algorithm.

4.3 CONTINUOUS CURVELET TRANSFORM

The Continuous Curvelet Transform has gone through two major revisions. The first Continuous Curvelet Transform (commonly referred to as the "Curvelet '99" transform now) used a complex series of steps involving the ridgelet analysis of the radon transform of an image. Performance was exceedingly slow. The algorithm was updated in 2003. The use of the Ridgelet Transform was discarded, thus reducing the amount of redundancy in the transform and increasing the speed considerably. In this new method, an approach of curvelets as tight frames is taken. Using tight frames, an individual curvelet has frequency support in a parabolic-wedge area of the frequency domain.

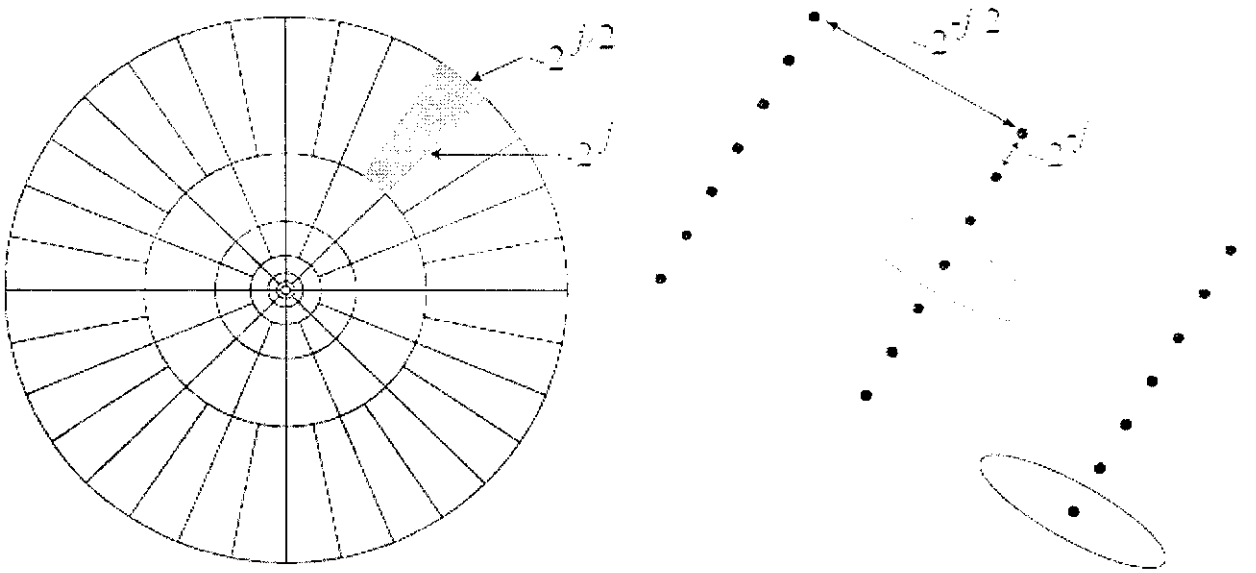

Fig.4.5 Continuous Curvelet Support in the Frequency Domain

The Figure on the left represents the induced tiling of the frequency plane. In Fourier space, curvelets are supported near a "parabolic" wedge, and the shaded area represents such a generic wedge. The Figure on the right schematically represents the spatial Cartesian grid associated with a given scale and orientation.

A sequence of curvelets is tight frames if there exists some value for A such that:

$$A\|f\|_{L^2}^2 = \sum_{j,l,k} \left|\left\langle f, \gamma_{j,l,k} \right\rangle\right|^2 : \forall f \in L^2 \qquad \text{-------- (4.9)}$$

Where each curvelet in the space domain is defined as:

$$\gamma_{j,l,k} = 2^{\frac{2j}{3}} \gamma(D_j R_\theta x - k_\delta) \qquad \text{-------- (4.10)}$$

Using the property of tight frames, the inverse of the curvelet transform is easily found as:

$$f = \sum_{j,l,k} \left\langle f, \gamma_{j,l,k} \right\rangle \gamma_{j,l,k} \qquad \text{-------- (4.11)}$$

(where, Dj = Parabolic Scaling matrix, R_θ = Rotation matrix, k = translation parameter)

4.4 DISCRETE CURVELET TRANSFORM

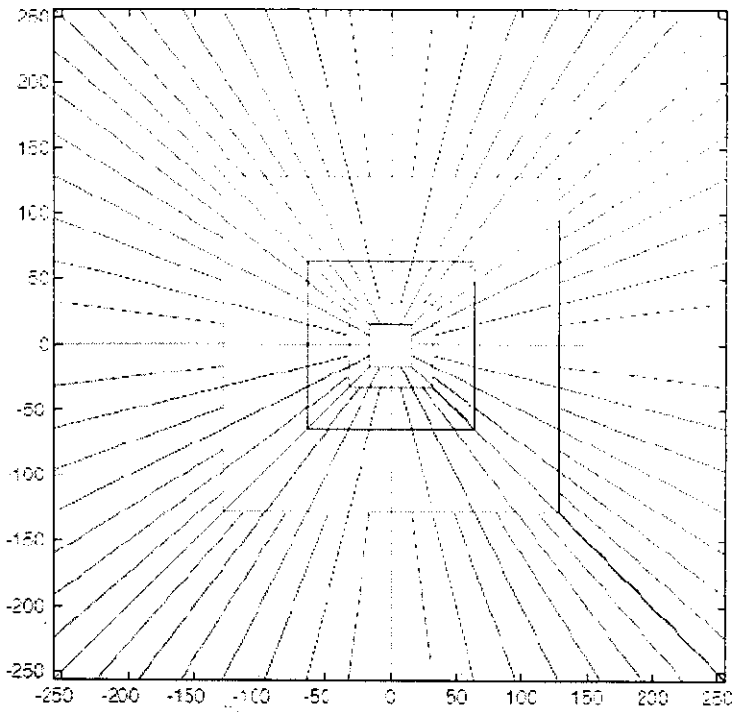

Fig.4.6 Digital Corona of the Frequency Domain

The curvelet transform has gone through two major revisions. The first generation curvelet transform used a complex series of steps involving the ridgelet analysis of radon transform of an image. The performance was exceeding slow. The second generation curvelet transform discarded the use of the ridgelet transform, thus reduced the amount of redundancy in the transform and increased the speed considerably.

Using the theoretical basis in (where the continuous curvelet transform is created), two separate digital (or discrete) curvelet transform (DCT) algorithms were introduced. The first algorithm is the Unequispaced Fast Fourier Transform (USFFT) Transform, where the curvelet coefficients are found by irregularly sampling the Fourier coefficients of an image. The second algorithm is the Wrapping transform, using a series of translations and a wraparound technique. Both algorithms having the same output, but the Wrapping Algorithm gives both a more intuitive algorithm and faster computation time. Because of this, the Unequispaced FFT method will be ignored in this paper with focus solely on the Wrapping DCT method.

The Discrete Curvelet Transform is defined as follows:

$$C(j,l,k) = \int f(w) U_j(S_{\theta_l}^{-1}) \exp[\, i\langle b, S_{\theta_l}^{-T} \rangle] dw = \int f\ (S_{\theta_l} w) U_j \exp[\, i\langle b, w \rangle] dw \qquad \text{-------- (4.12)}$$

- The Wrapping Algorithm has faster computation time.
- The two implementations essentially differ by the choice of spatial grid used to translate curvelets at each scale and angle.

4.4.1 Fast Discrete Curvelet Transform – Wrapping

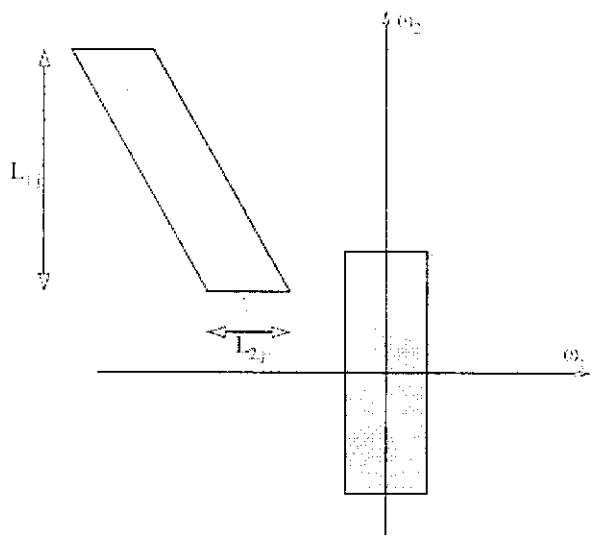

Fig. 4.7 Wrapping Data, Initially inside a Parallelogram, into a Rectangle by Periodicity.

The angle θ is here in the range ($\pi/4$, 3 π /4). The black parallelogram is the tile $P_{j,l}$ which contains the frequency support of the curvelet, whereas the gray parallelograms are the replicas resulting from periodization. The rectangle is centered at the origin. The wrapped ellipse appears "broken into pieces" but as we shall see, this is not an issue in the periodic rectangle, where the opposite edges are identified

4.4.2 FDCT Architecture

- Frequency space is divided into dyadic annuli based on concentric squares.
- Each annulus is subdivided into trapezoidal regions. In the USFFT version, the discrete Fourier transform, viewed as a trigonometric polynomial, is sampled within each parallelepiped region according an equispaced grid aligned with the axes of the

parallelogram. Hence, there is a different sampling grid for each scale/orientation combination. The wrapping version, instead of interpolation, uses periodization to localize the Fourier samples in a rectangular region in which the IFFT can be applied. For a given scale, this corresponds only to two Cartesian sampling grids, one for all angles in the east-west quadrants, and one for the north-south quadrants.

- Both forward transforms are specified in closed form, and are invertible (with inverse in closed form for the wrapping version).
- The design of appropriate digital curvelets at the finest scale, or outermost dyadic corona, is not straightforward because of boundary/periodicity issues.
- The transforms are cache-aware: all component steps involve processing n items in the array in sequence, e.g., there is frequent use of 1D FFTs to compute n intermediate results simultaneously.

4.4.3 FDCT – Wrapping Algorithm

The algorithm for the fast discrete curvelet transform (FDCT) can then be summarized as follows:

1. Apply the 2D FFT and obtain Fourier samples

$$f[n_1, n_2], -n/2 \le n_1, n_2 \le n/2 \qquad \text{-------- (4.13)}$$

2. For each scale j and angle l, form the product

$$U_{j,l}[n_1, n_2] f[n_1, n_2] \qquad \text{-------- (4.14)}$$

3. Wrap this product around the origin and obtain

$$f_{j,l}[n_1, n_2] = W(U_{j,l} \cdot f)[n_1, n_2] \qquad \text{------- (4.15)}$$

Where the range for n_1 and n_2 is now $0 \le n_1 < L_{1,j}$ and $0 \le n2 < L_{2,j}$ (for θ in the range$(-\pi/4, \pi/4)$).

4. Apply the inverse 2D FFT, hence collecting the discrete coefficients $c^D(j, l, k)$.

This chapter explains the basics and needs of discrete curvelet transform and its wrapping algorithm.

CHAPTER 5

PROPOSED ALGORITHM

5.1 IMAGE FUSION ALGORITHM BASED ON DWT AND DCT

Images can be fused in three levels, namely pixel level fusion, feature level fusion and decision level fusion. Pixel level fusion is adopted in this paper. We can take operation on pixel directly, and then fused image could be obtained. We can keep as more information as possible from source images. Because Wavelet Transform takes block base to approach the singularity of C^2, thus isotropic will be expressed; geometry of singularity is ignored. Curvelet Transform takes wedge base to approach the singularity of C^2. It has angle directivity compared with Wavelet, and anisotropy will be expressed. When the direction of approachable base matches the geometry of singularity characteristics, curvelet coefficients will be bigger.

Pixel level fusion is adopted in this method. We can take operation on pixel directly, and then fused image could be obtained. We can keep as more information as possible from source images.Wavelet Transform is used to decompose original images into proper levels. One low-frequency approximate component and three high-frequency detail components will be acquired in each level.

Curvelet Transform of individual acquired low frequency approximate component and high frequency detail components from both of images, neighbourhood interpolation method is used. Inverse transformation of coefficients after fusion, the reconstructed images will be fusion images.

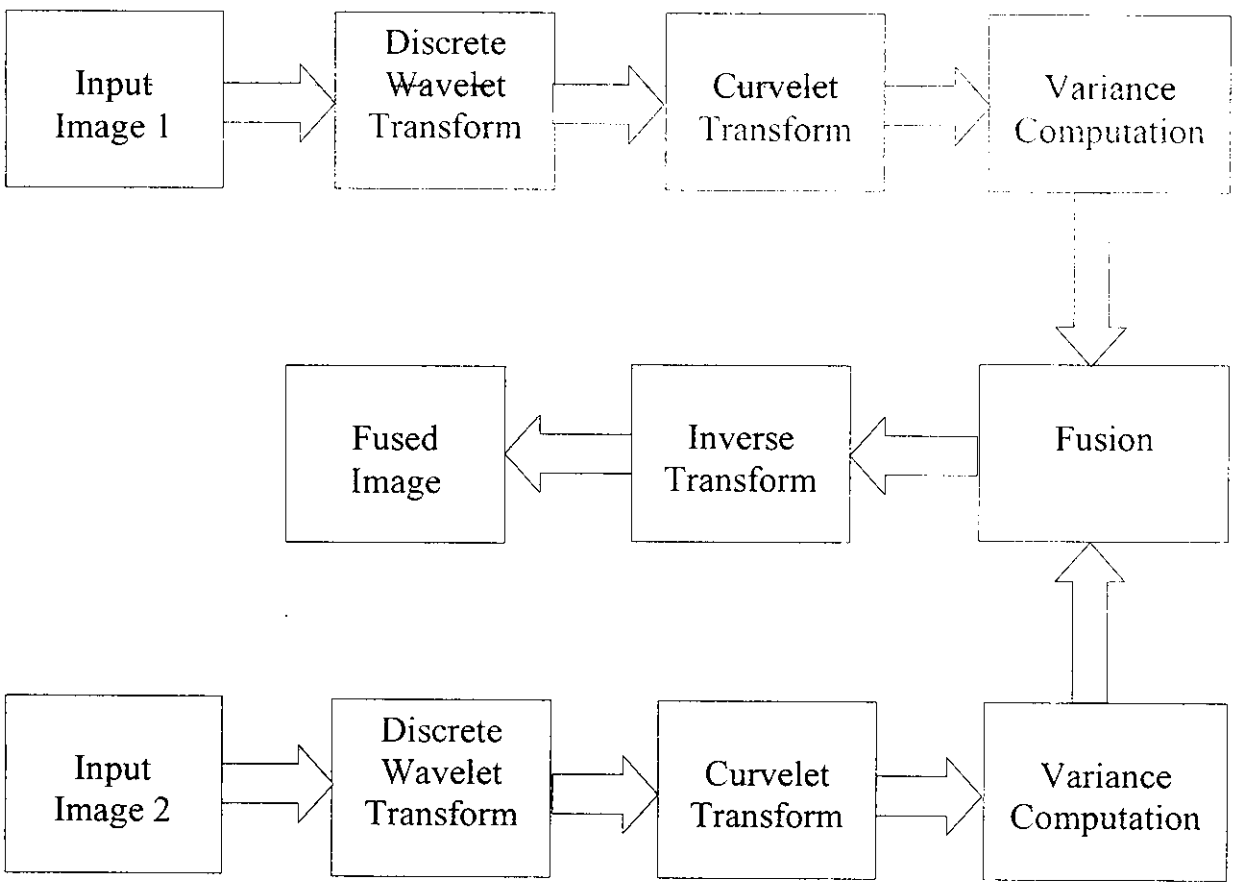

Fig. 5.1 Block Diagram of Image Fusion

5.1.1 Methodology

First, we need pre-processing and then cut the same scale from awaiting fused images according to selected region. Subsequently, we divide images into sub-images which are different scales by Wavelet Transform. Afterwards, local Curvelet Transform of every sub-image should be taken; its sub-blocks are different from each other's on account of scales' change. The steps of using Curvelet Transform to fuse two images are as follows:

- Resample and registration of original images, we can correct original images and distortion so that both of them have similar probability distribution. Then Wavelet coefficient of similar component will stay in the same magnitude.
- Using Wavelet Transform to decompose original images into proper levels. One low-frequency approximate component and three high-frequency detail components will be acquired in each level.
- Curvelet Transform of individual acquired low frequency approximate component and high frequency detail components from both of images, neighborhood interpolation method is used and the details of gray can't be changed.
- According to definite standard to fuse images, local area variance is chose to measure definition for low frequency component. First, divide low-frequency $C_{j0}(k_1,k_2)$ into individual foursquare sub-blocks which are $N_1 \times M_1$ (3×3 or 5×5), then calculate local area variance of the current sub-block:

$$STD = \sqrt{\frac{\sum_{i=-(N_1-1)/2}^{(N_1-1)/2} \sum_{}^{(M_1-1)/2} [c_{j_0}(k_1+i,k_2+j)-c_{j_0}(k_1,k_2)]^2}{N_1 \times M_1}}$$

-------- (5.1)

Here, $\hat{C}_{j0}(k_1,k_2)$ stands for low-frequency coefficient mean of original images. If variance is bigger, it shows that the local contrast of original image is bigger, that means clearer definition. It is expressed as follows:

$$C_{j0}^{F}(k_1,k_2)=\begin{Bmatrix} C_{j0}^{A}(k_1,k_2), STD^{A} \geq STD^{B} \\ C_{j0}^{B}(k_1,k_2), STD^{A} \leq STD^{B} \end{Bmatrix}$$

-------- (5.2)

Regional activity $E_{j,l}(k_1,k_2)$ is defined as a fusion standard of high-frequency components. First, divide high-frequency sub-band into sub-blocks, then calculate regional activity of sub-blocks.

$$E_{j,l}(k_1,k_2)=\sum_{i=-(N_1-1)/2}^{(N_1-1)/2}\sum_{j=-(M_1-1)/2}^{(M_1-1)/2}[C_{j,l}(k_1+i,k_2+j)]^2$$

-------- (5.3)

In which, $N_1 \times M_1$ means 3×3, 5×5 and so on

- Inverse transformation of coefficients after fusion, the reconstructed images will be fusion images.

5.2 PARAMETERS OF EVALUATION RESULT

There are two methods to evaluation the fusion result, which are subjective evaluation and objective evaluation. Subjective evaluation is based on the knowledge and experience of vision, and it is very easy. However, it is lack of objectivity and different people will come to a different conclusion. In order to the quantitative analysis, this paper makes use of some statistical parameters to evaluate the fusion result, such as correlation coefficient, information entropy and error RMS value.

Correlation coefficient: Correlation Coefficient is used to measure strength of the linear relationship between pixels of an image. Its value lies between 0 to1. Correlation coefficient reflects the relevance of image X and image Y.

$$r = \frac{\sum_m \sum_n (A_{mn} - \overline{A})(B_{mn} - \overline{B})}{\sqrt{\sum_m \sum_n (A_{mn} - \overline{A})^2 \sum_m \sum_n (B_{mn} - \overline{B})}}$$

-------- (5.4)

m, n are number of rows and columns of input image.

$\overline{A}$ = mean value of A.

$\overline{B}$ = mean value of B.

The correction coefficient between the original and fused image shows similarity in the small structures between the original and synthetic images.

Entropy: Entropy is a measure of disorder. Maximum entropy gives the smoothest and simplest image. It can be used to characterize the texture of an input image. Information entropy can measure the information quantity of each image and it is defined as:

$$H(X) = -\sum_{i=0}^{A-1} p_i . \log_2 (p_i)$$ -------- (5.5)

where, p_i - probability of the pixels with gray

A - the image gray series

Root Mean Square (RMS): Root Mean Square (RMS) value is the average error value of an image. Generally RMS is defined as

RMS for an image = normalized value of n/ $\sqrt{length(n)}$ -------- (5.6)

where, n is the input image

5.3 EXPERIMENTAL RESULTS AND ANALYSIS

5.3.1 Multi Focus Image Fusion

We use multi-focus images after standard testing. Fig. 5.2(a) shows left-focus image, the outline of small clock looks clear. Fig. 5.2(b) shows right-focus image, the outline of the big clock looks clear. Two fusion algorithms are adopted in this paper to contrast fusion effects. We separately use Discrete Wavelet Transform (DWT), Discrete Fast Curvelet Transform (DFCT) along with DWT which is proposed in this paper. Different fusion standard is used in different sections. Average operator is used as a fusion standard for low-frequency sub-band.

Choosing the fusion operator based the biggest absolute value is used as a fusion standard for three high-frequency sub-band from the highest scale. Choosing the fusion operator based the biggest local area variance is used as a fusion standard for high-frequency sub-band from other scales.

Fig. 5.2(c) and Fig. 5.2(d) shows both the algorithms acquire good fusion results, focus difference has been eliminated and definition of original images has been proved. The result of DWT looks worse by contrast; we can see evident faintness in edges and also false contours of edges appear. We acquire the best subjective effect in Fig. 5.2(d). The fused image is the clearest, and detail information is kept as more.

The entropy of fused image, correlation coefficient and RMS error to evaluate the fused quality, it is expressed as Table 5.1. In the same group of experiments, if Entropy of fused image is bigger, or correlation coefficient approach one more closer, RMS is smaller. It shows that the fusion methods adopted is better.

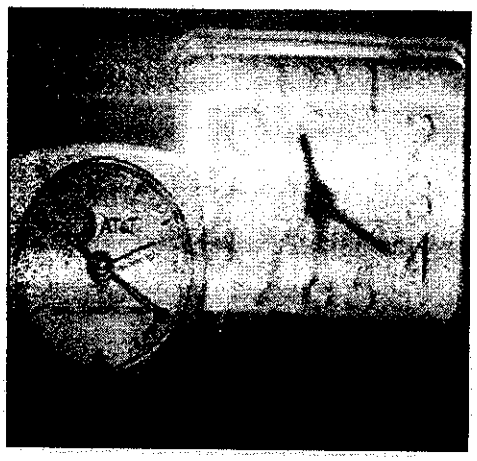

Fig. 5.2(a) Left Focus Image

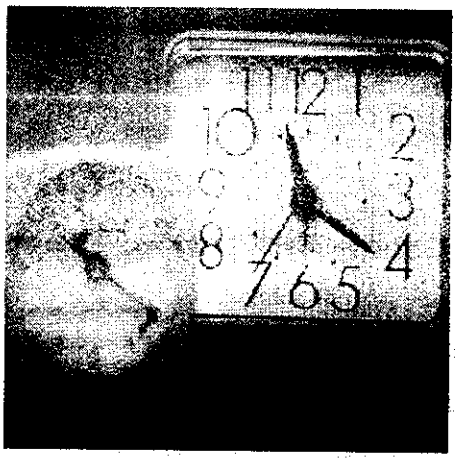

Fig. 5.2(b) Right Focus Image

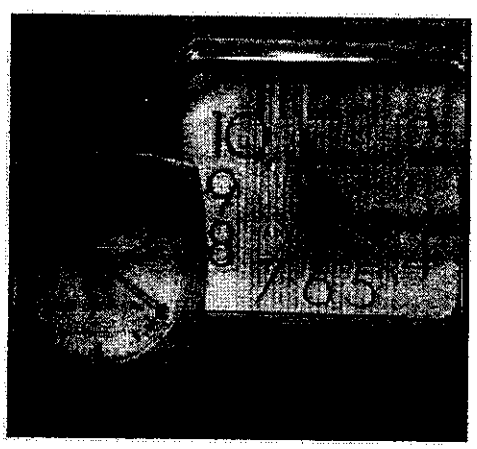

Fig. 5.2(c) Fused Image of DWT

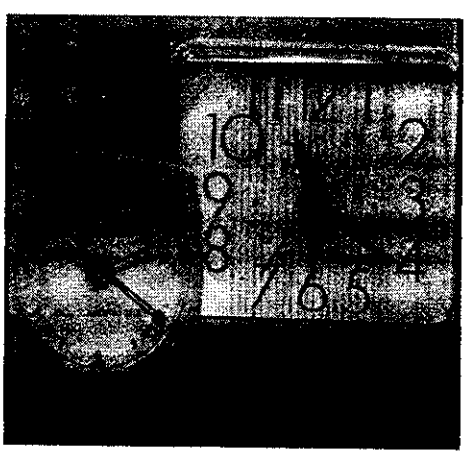

Fig. 5.2(d) Fused Image of DWT and DCT

Table 5.1 Evaluation of Multifocus Image Fusion Results

	Correlation Coefficient	Entropy (J/K)	RMS
Blur 1 (left focus image)	0.9998	7.3175	9.6540
Blur 2 (right focus image)	0.8300	7.2564	9.6540
Fused Image Wavelet Transform	0.9989	7.3205	9.9974
Fused Image Curvelet Transform.	1.0000	7.5629	10.000

In the above Table entropy, RMS and correlation coefficient values for the fused image based on wavelet and curvelet transforms are tabulated. It is evident from the Table that image fusion using curvelet transform gives better correlation coefficient and entropy. The RMS value is slightly increased because of the high information content in the image.

Fig. 5.3(a) shows left-focus image, the outline of small box looks clear. Fig. 5.3(b) shows right-focus image, the outline of the large box looks clear.

Fig. 5.3(c) and Fig. 5.3(d) shows both the algorithms acquire good fusion results, focus difference has been eliminated and definition of original images has been proved. The result of DWT looks worse by contrast; we can see evident faintness in edges and also false contours of edges appear. We acquire the best subjective effect in Fig. 5.2(d). The fused image is the clearest, and detail information is kept as more.

The entropy of fused image, correlation coefficient and RMS to evaluate the fused quality, it is expressed as Table 5.2.

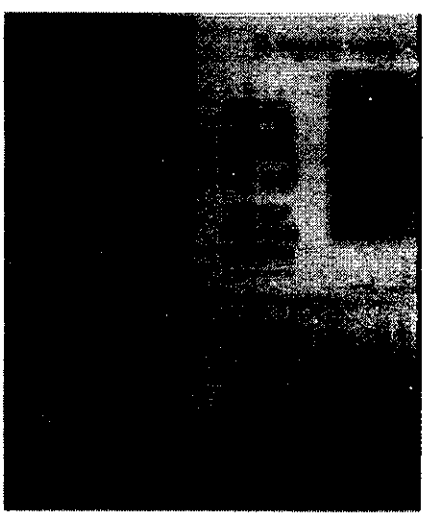

Fig. 5.3(a) Left Focus Image

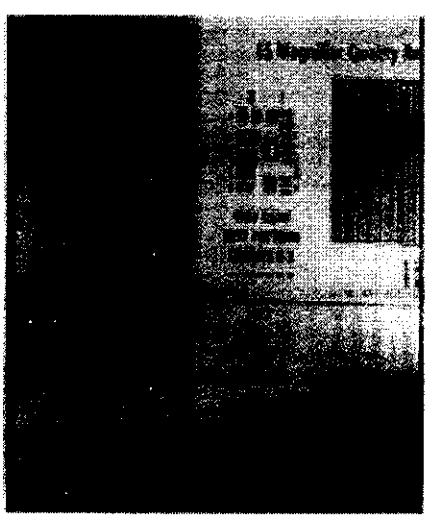

Fig. 5.3(b) Right Focus Image

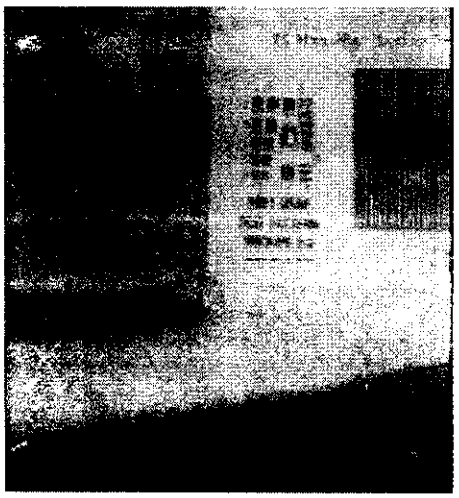

Fig. 5.3(c) Fused Image of DWT

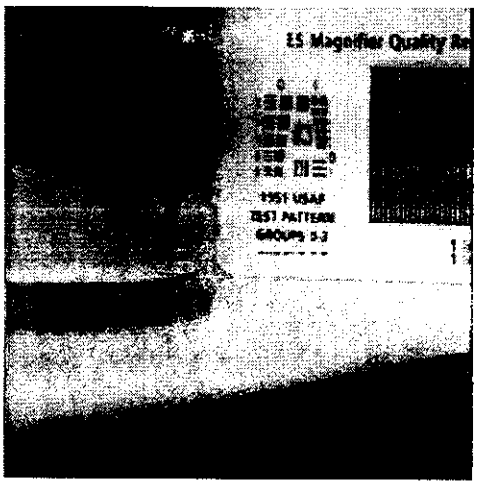

Fig. 5.3(c) Fused Image of DWT and DCT

Table 5.2 Evaluation of Multifocus Image Fusion Results

	Correlation Coefficient	Entropy (J/K)	RMS
Blur 1 (left focus image)	0.9538	7.0858	9.1534
Blur 2 (right focus image)	0.9644	7.1051	9.1515
Fused Image Wavelet Transform	0.9996	7.1067	9.4382
Fused Image Curvelet Transform.	0.9999	7.3920	9.1837

Fig. 5.4(a) shows lena1 image, in that image one type of information is loss. Fig. 5.3(b) shows lena 2 image, in that other type of information is loss.

Fig. 5.4(c) and fig. 5.4(d) shows both the algorithms acquire good fusion results, focus difference has been eliminated and definition of original images has been proved. The result of DWT looks worse by contrast; we can see evident faintness in edges and also false contours of edges appear. We acquire the best subjective effect in Fig. 5.2(d). The fused image is the clearest, and detail information is kept as more. The entropy of fused image, correlation coefficient C_{cc} and rms error E_{rms} to evaluate the fused quality, it is expressed as Table 5.3.

Fig. 5.5(a) Lena 1

Fig. 5.5(b) Lena 2

Fig. 5.5(c) Fused Image of DWT

Fig. 5.5(c) Fused Image of DWT and DCT

Table 5.3 Evaluation of Multifocus Image Fusion Results

	Correlation Coefficient	Entropy (J/K)	RMS
Lena 1	0.8889	7.4726	6.4239
Lena 2	0.8890	7.4731	6.4267
Fused Image Wavelet Transform	0.8886	7.4761	6.4547
Fused Image Curvelet Transform.	0.8888	7.6178	6.1395

5.3.2 Satellite Image Fusion

Large number of images is provided by satellite with different spatial resolution and spectral resolution. Fig5.5 (a) shows lower spatial resolution multispectral image (high spectral resolution) Fig5.5 (b) shows high spatial resolution panchromatic image (poor spectral resolution).

Fig5.5 (c) shows fused image obtained by using discrete wavelet transform. It provides the image have acceptable spatial and spectral characteristics. Fig5.5 (d) shows fused image obtained by using Curvelet Transform. It provides the image have good spatial and spectral characteristics. Fused image's performance is tabulated.

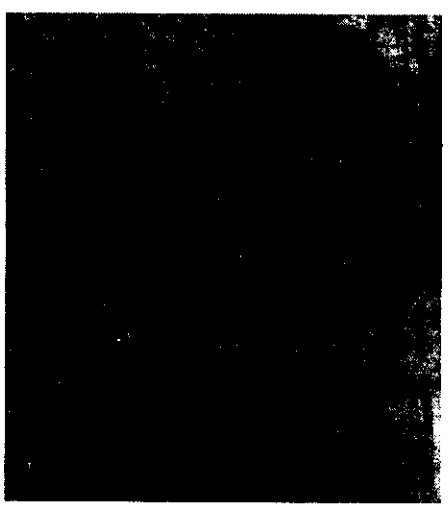

Fig. 5.5(a) Multi Spectral Image

Fig. 5.5(b) Panchromatic Image

Fig. 5.5(c) Fused Image of DWT

Fig. 5.5(d) Fused Image of DWT and DCT

Table 5.4 Evaluation of Satellite Image Fusion Results

	Correlation Coefficient	Entropy (J/K)	RMS
Multispectral Image	0.7987	6.6282	5.4053
Panchromatic Image	0.8055	7.3206	9.7376
Fused Image Wavelet Transform	0.8384	7.3284	10.0638
Fused Image Curvelet Transform.	0.8698	7.5111	9.8621

5.3.3 Complementary Image Fusion

In medicine, CT and MRI image both are tomography scanning images. The have different features. Fig. 5.6(a) shows CT image, in which image brightness related to tissue density, brightness of bones is higher, and some soft tissue can't been seen in CT images. Fig. 5.6(b) shows MRI image, here brightness of soft tissue is higher, and bones can't be seen. There is complementary information in these images. The two methods of fusion forenamed in medical images are used and adopt the same fusion standards. Fig. 5.6(c) and (d) separately shows results and the data of results is expressed as Table 5.5.

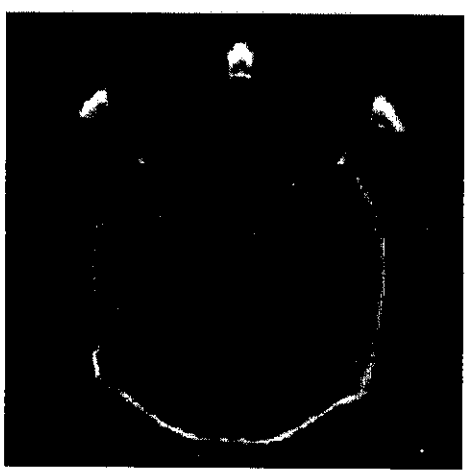

Fig. 5.6(a) CT Image

Fig. 5.6(b) MRI Image

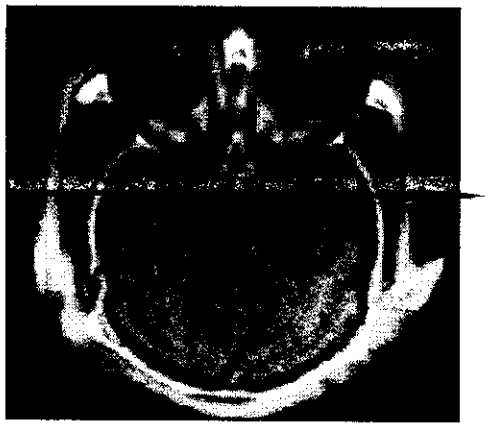

Fig. 5.6(c) Fused Image of DWT

Fig. 5.6(c) Fused Image of DWT and DCT

Table 5.5 Evaluation of Complementary Image Fusion Results

	Correlation Coefficient	Entropy (J/K)	RMS
CT Image	0.9076	6.6328	4.0240
MRI Image	0.9580	2.0325	1.3274
Fused Image Wavelet Transform	0.8884	6.7500	4.3386
Fused Image Curvelet Transform.	1.0000	6.7577	4.3380

The quality of the fused satellite multi focused and medical images are analyzed using the parameters like Entropy, RMS, correlation coefficient.

CHAPTER 6

CONCLUSION

Image fusion is performed by wavelet and curvelet transform. In the wavelet transform based image fusion, edge information and direction of the image is lost. This limitation is overcome by applying curvelet transform. The fused image which is obtained through curvelet based image fusion technique has better entropy, root mean square value, correlation coefficient value when compared to the existing wavelet based fusion technique. Line singularities are effectively taken care by curvelet transform.

The implementation of curvelet transform based image fusion is still in a preliminary stage. However the results obtained so far suggest that this approach may be useful for several image fusion applications.

REFERENCES

[1] F. Laliberte; L. Gagnon; "Registration and fusion of retinal images – An evaluation study"; IEEE Transactions on Medical Imaging; 2003, V 22, N5, P 661-673.

[2] J.-L. Starck, F. Murtagh and R. Gastaud, "A new entropy measure basedon the wavelet transform and noise modeling", IEEE Transactions on Circuitsand Systems II: Analog and Digital Signal Processing, 45, 1118-1124, 1998

[3] Z. Zhang, Investigations of Image Fusion. PHD dissertation, Lehigh University,Bethlehem, PA, May 1999.

[4] R. A. Redner and H. F. Walker, "Mixture densities, maximum likelihood and the EMalgorithm," SIAM Review, vol. 26, no. 2, pp. 195-239, April 1984.

[5] D. A. Fay, A. M. Waxman, M. Aguilar, D. B. Ireland, J. P. Racamato, W. D. Ross, W. W. Streilein,and M. I. Braun, "Fusion of multi- sensor imagery for night vision: Color visualization, target learningand search," in Proc. 3rd Int. Conf. Information Fusion, Paris, 2000, pp. 215-219.

[6] Steidl, G., Weickert, J., Brox, T., P. Mrazek, and Welk, M.: "On the equivalence of soft wavelet shrinkage, total variation di®usion, total variation regularization, and SIDEs", SIAM Journal on Numerical Analysis, 2004, 42(2), pp.686-713.

[7] Chao Rui, Zhang Ke, Li Yan-jun, 'An image fusion algorithm using Wavelet Transform', Chinese Journal of Electronics, 2004, 32(5), pp 750-753.

[8] Li, H., Manjunath, B.S., Mitra, S.K., 'Multisensor image fusion using the Wavelet Transform'. Graphical Models Image Process. 1995, 57 (5), pp 235–245.

[9] Li, S., Wang, Y., 'Multisensor image fusion using discrete MultiWavelet Transform'. In: Proc. 3rd Internat. Conf. on VisualComputing, 2000, pp. 93–103.

[10] Li, H., Manjunath, B.S., Mitra, S.K., 'Multisensor image fusion using the Wavelet Transform'. Graphical Models Image Process, 1995, 57 (5), pp. 235–245.

[11] E. J. Candes, D. L. Donoho. 'Curvelets: A surprisingly effective nonadaptive representation for objects with edges'. In: C. Rabut A. Cohen, L. L. Schumaker. Curves and Surfaces. Nashville, TN: Vanderbilt University Press, 2000, pp. 105-120.

[12] E. J. Candes,D. L. Donoho, 'New tight frames of curvelets andoptimal representations of objects with singularities'. Commun. On Pure and Appl. Math.2004, 57(2), pp. 219-266.

[13] E. J. Candes, L. Demanet, D.L. Donoho et al.. 'Fast Discrete Curvelet Transforms'. Applied and Computational Mathematics. California Institute of Technology 2005.1.

[14] LiHui-hu, i GuoLe, i LiuHang,'Research on image fusion based onthe second generation curvelet transform'. Acta Optica Sinica, 2006, 26(5), pp. 657-662.

[15] Huang Xishan, Chen Zhe. 'A wavelet based scene image fusion algorithm'. Proceedings of EEE TENCON 2002. Piscateway, USA , IEEE Press, 2002, pp. 602-605.

[16] Starck J. L, Candes E. J, Donoho D. L, 'The Curvelet Transform for image denoising'. IEEE Trans Image Process, 2002, 11(6), pp. 670-684.

[17] Steidl, G., Weickert, J., Brox, T., P. Mrazek, and Welk, M.: "On the equivalence of soft wavelet shrinkage, total variation di®usion, total variation regularization, and SIDEs", SIAM Journal on Numerical Analysis, 2004, 42(2), pp.686-713.

[18] L. Sendur, I.W. Selesnick, Bivariate shrinkage functions for wavelet based denoising exploiting interscale dependency, IEEE Trans. Signal Pr pocess. 50 (11) (2002) 2744–2756.

ICCOS '11

Karunya UNIVERSITY

(Karunya Institute of Technology and Sciences)
Declared as Deemed to be University Under sec. 3 of the UGC Act, 1956
Karunya Nagar, Coimbatore 641 114. India

Department of Electronics and Communication Engineering

CERTIFICATE

This is to certify that Dr/Mr/Ms/Mrs. A. Kanagasabapathy of Kumaraguru College of Technology, Coimbatore has ~~participated~~ presented a paper titled "Image fusion based on Wavelet transform" in the International Conference on "Communication and Signal Processing (ICCOS '11)" on 17th & 18th March 2011 organized by the School of Electrical Sciences, Department of Electronics and Communication Engineering, Karunya University, Coimbatore, India.

Dr. A. Ravi Sankar
Convener

Dr. (Mrs.) Anne Mary Fernandez
Patron

Dr. Paul P. Appasamy
Patron

KUMARAGURU COLLEGE OF TECHNOLOGY

(An Autonomous Institution Affiliated to Anna University of Technology, Coimbatore)

COIMBATORE - 641049, TAMIL NADU, INDIA.

CERTIFICATE

CITEL 2011

This is to certify that Mr./~~Ms.~~ A. KANAGASABAPATHY, ME [COMMUNICATION SYSTEMS] KUMARAGURU COLLEGE OF TECHNOLOGY, COIMBATORE has ~~attended~~ / presented a paper titled IMAGE FUSION BASED ON WAVELET AND CURVELET TRANSFORM in the 3rd National Conference on **COMMUNICATION, INFORMATION AND TELEMATICS (CITEL 2011)** on 3rd & 4th March 2011, organized by the Department of Electronics and Communication Engineering, Kumaraguru College of Technology, Coimbatore.

Dr. Karpagavalli Ramachandran
Convener

Dr. S. Ramachandran
Principal

Dr. J. Shanmugam
Director